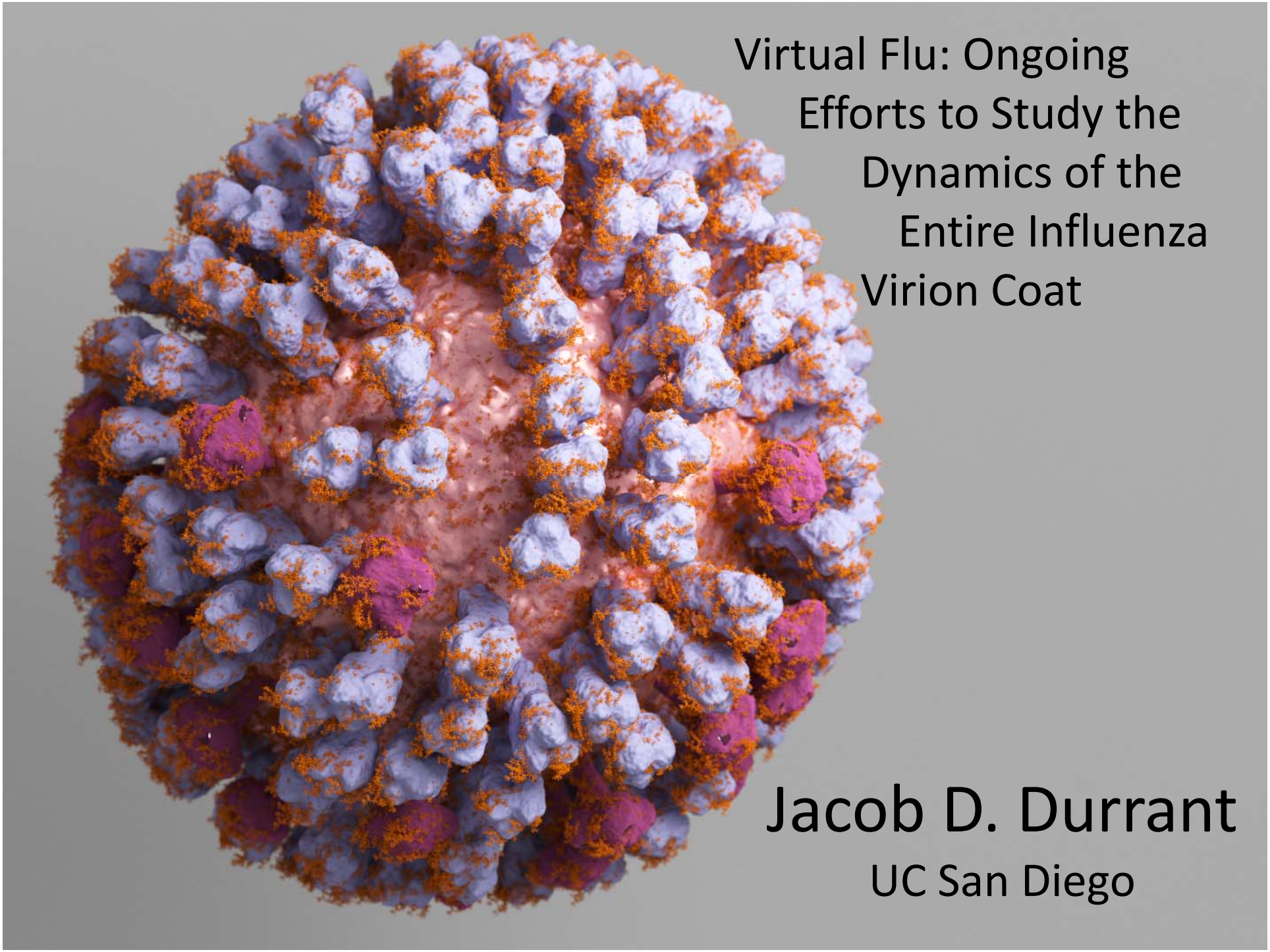

Virtual Flu: Ongoing Efforts to Study the Dynamics of the Entire Influenza Virion Coat

Jacob D. Durrant

UC San Diego

NBCR

Funded by a grant from the
National Institutes of Health
National Institute of General Medical Sciences

Here representing Dr. Rommie E. Amaro, NBCR's Executive Director

Virtual Flu

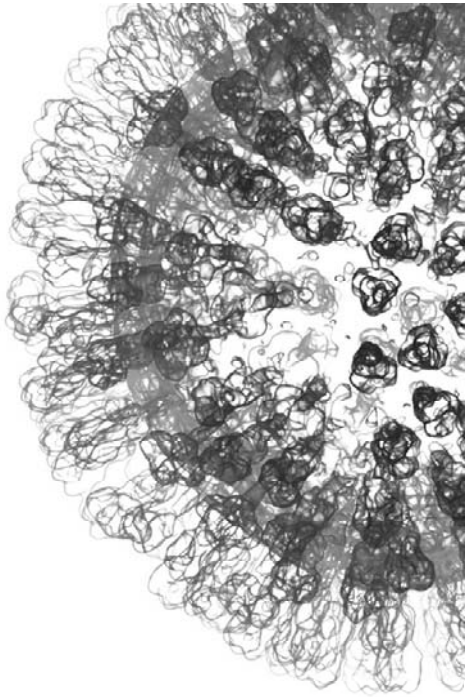

- Introduction
- Model Construction / Tool Development
- Ongoing simulations
- Utility

Influenza

- Influenza viruses are responsible for seasonal flu that takes about 500,000 lives a year.
- An influenza *pandemic* occurs about three times a century and can be far more devastating.
  - The 1918 Spanish flu may have killed as many as 100 million people.

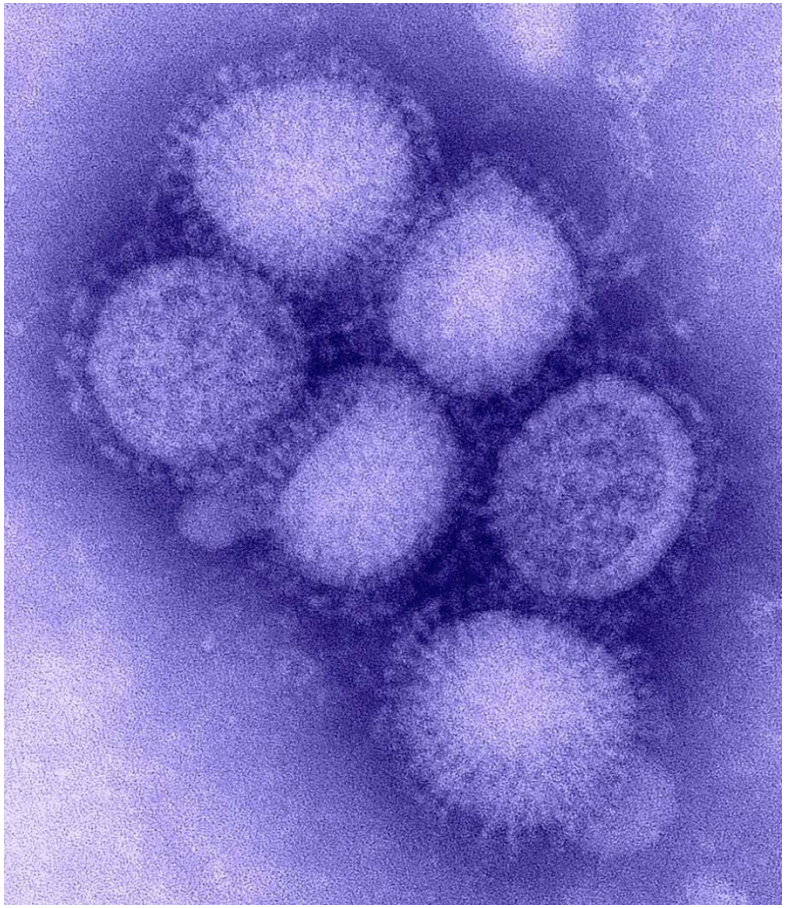

CDC Influenza Labratory

Influenza (Seasonal), World Health Organization, April 2009. Retrieved 13 February 2010.

Barry, John M. (2005). "1 The Story of Influenza: 1918 Revisited: Lessons and Suggestions for Further Inquiry". In Knobler SL, Mack A, Mahmoud A, Lemon SM. The Threat of Pandemic Influenza: Are We Ready? Workshop Summary (2005). The National Academies Press. pp. 60–61.

Infection at the Viral Surface Coat

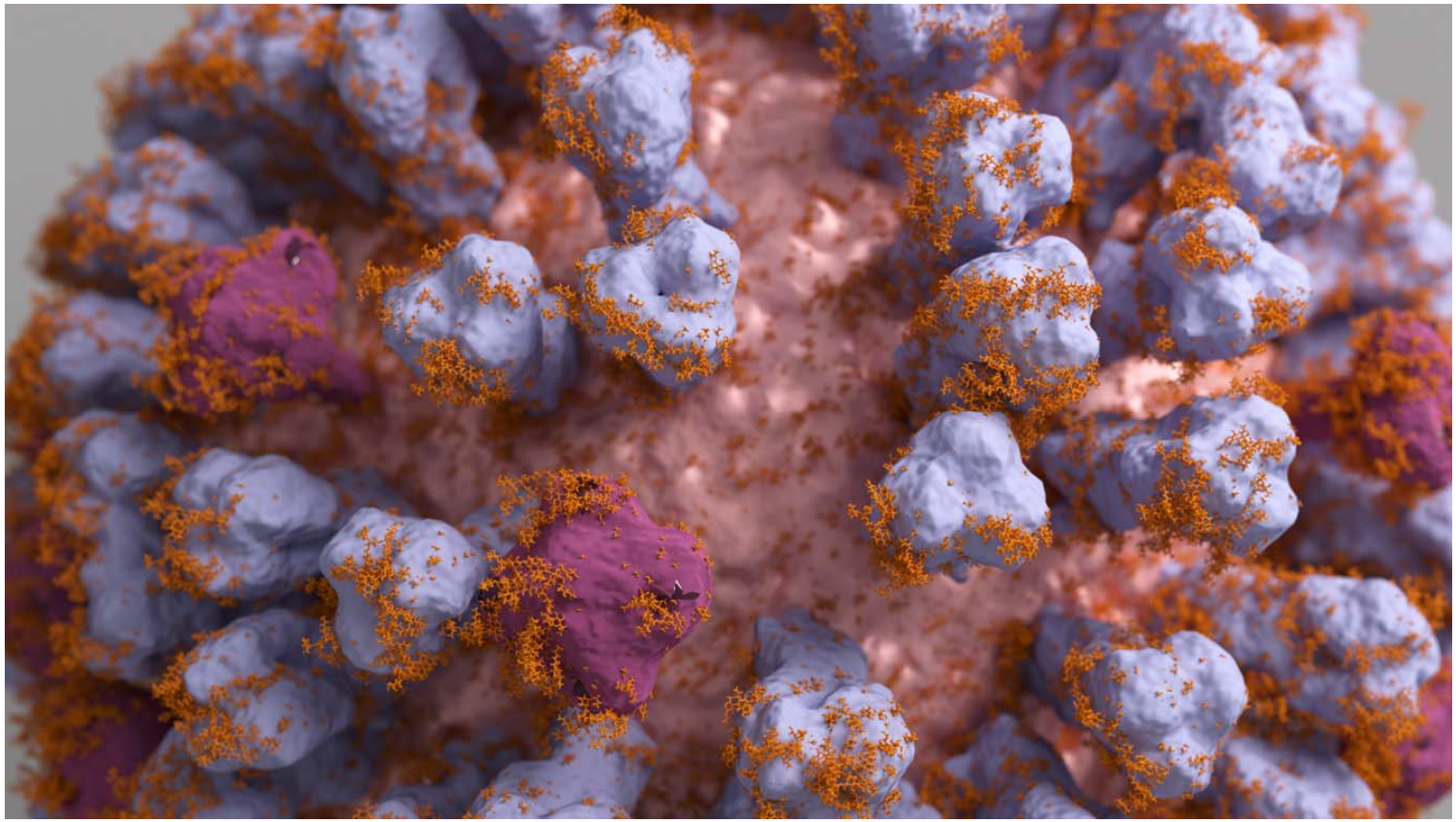

- HA binds to sialic-acid residues attached to cell-bound glycoproteins and glycolipids.

Infection at the Viral Surface Coat

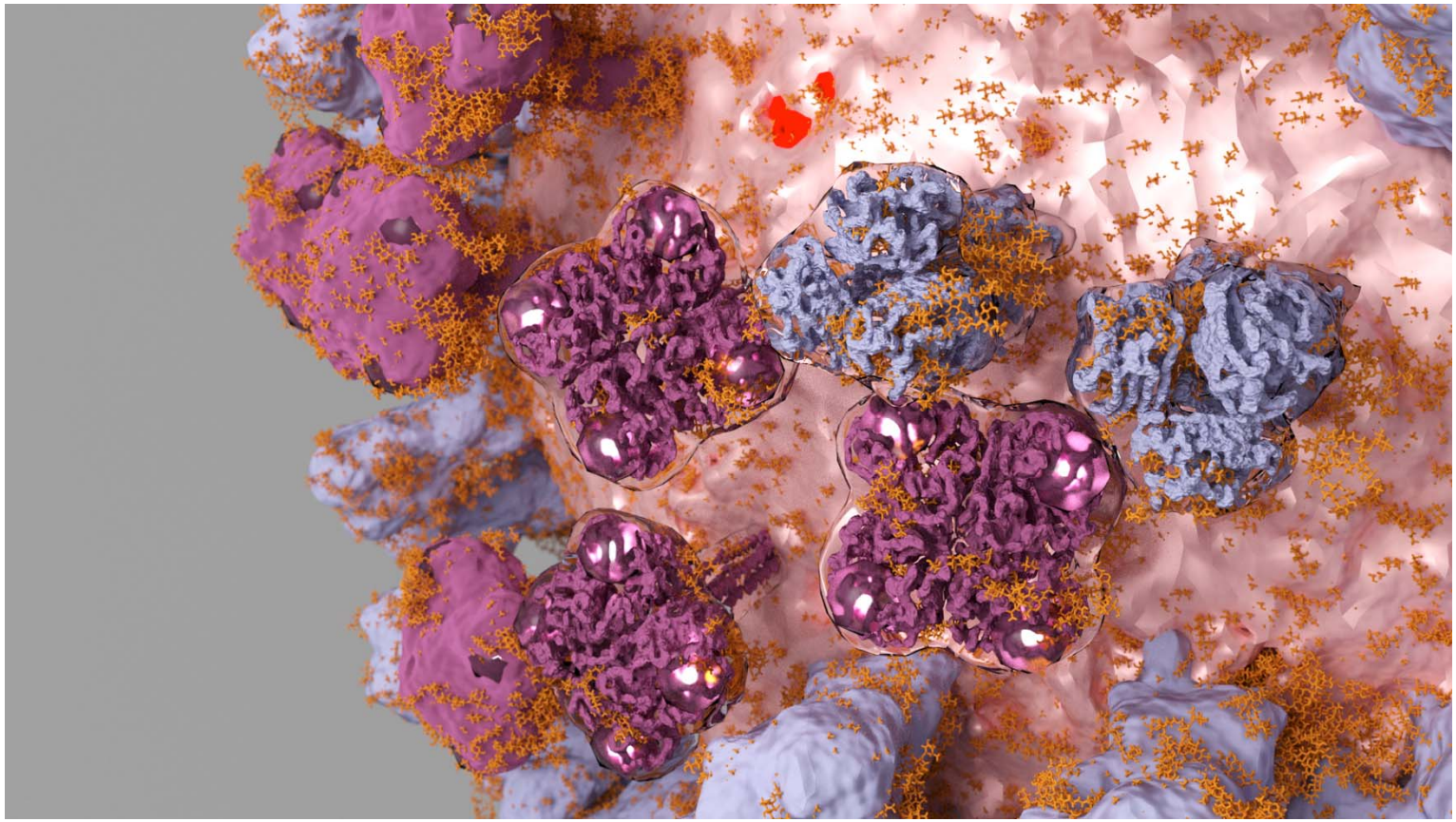

- NA cleaves these sialylated oligosaccharide receptors, releasing the newly formed viral progeny.

Virtual Flu

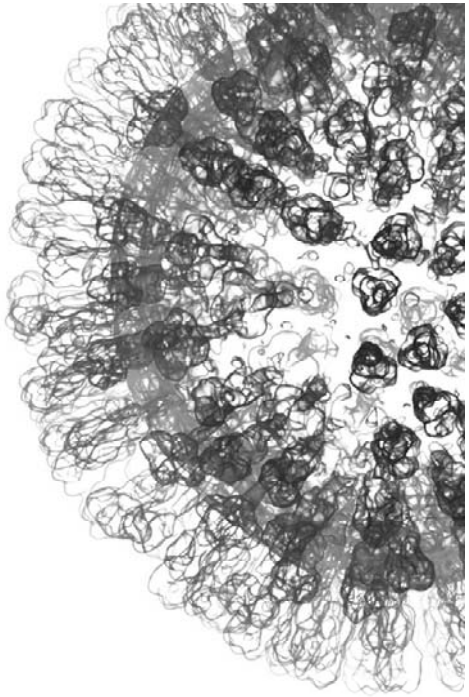

- Introduction
- **Model Construction / Tool Development**
- Ongoing simulations
- Utility

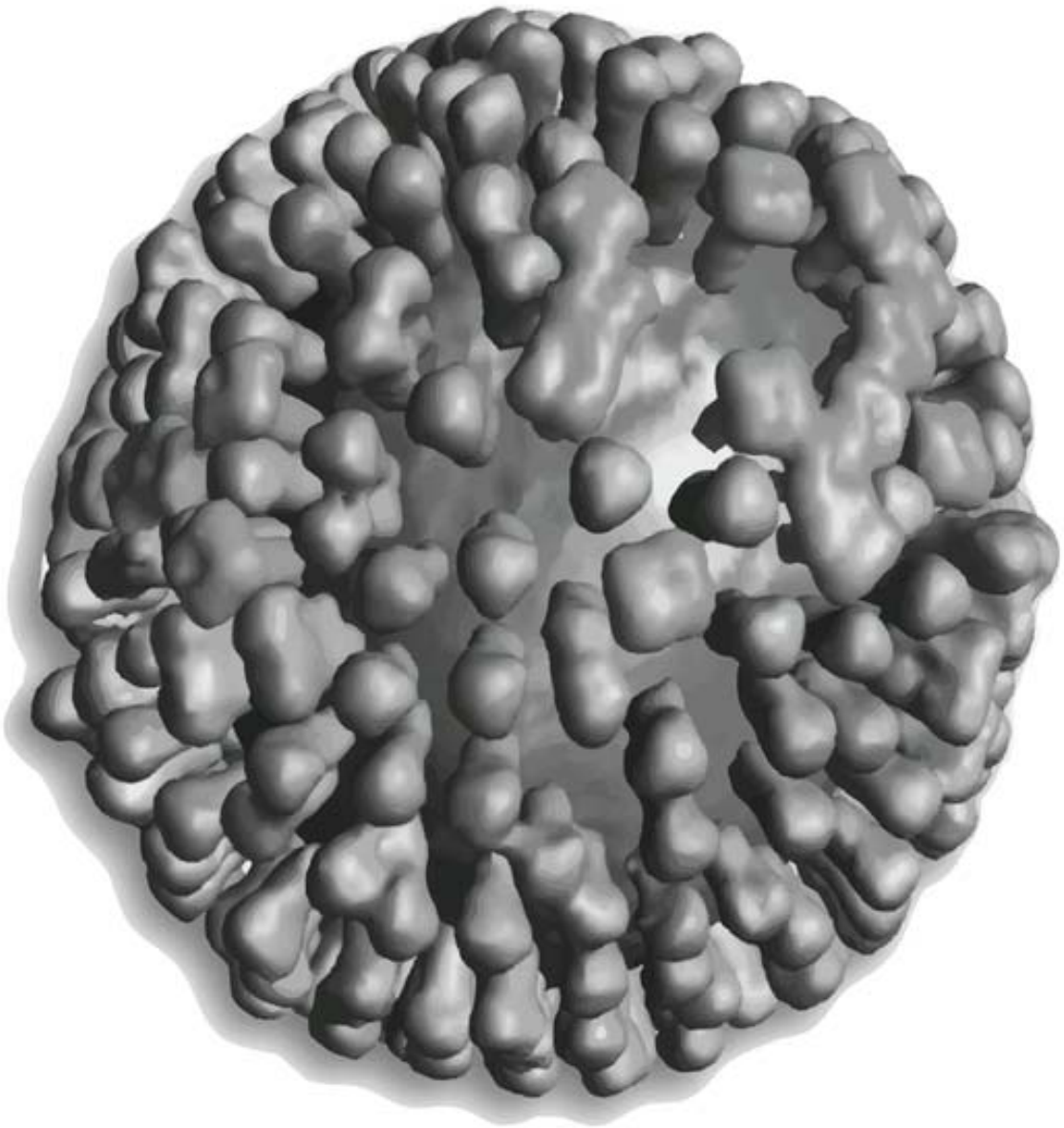

Tool Development

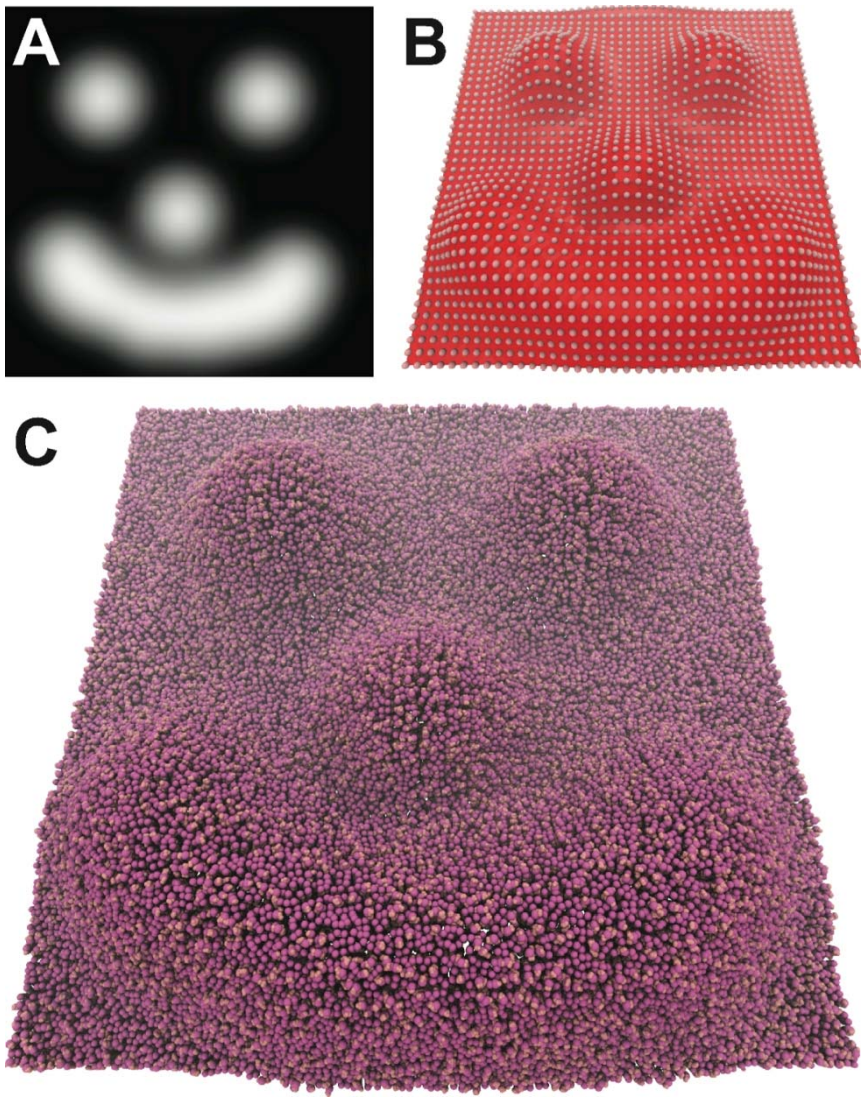

LipidWrapper: a tool to wrap fully atomic lipid membranes around arbitrary geometries

Durrant & Amaro, PLOS Comp Bio (2014).

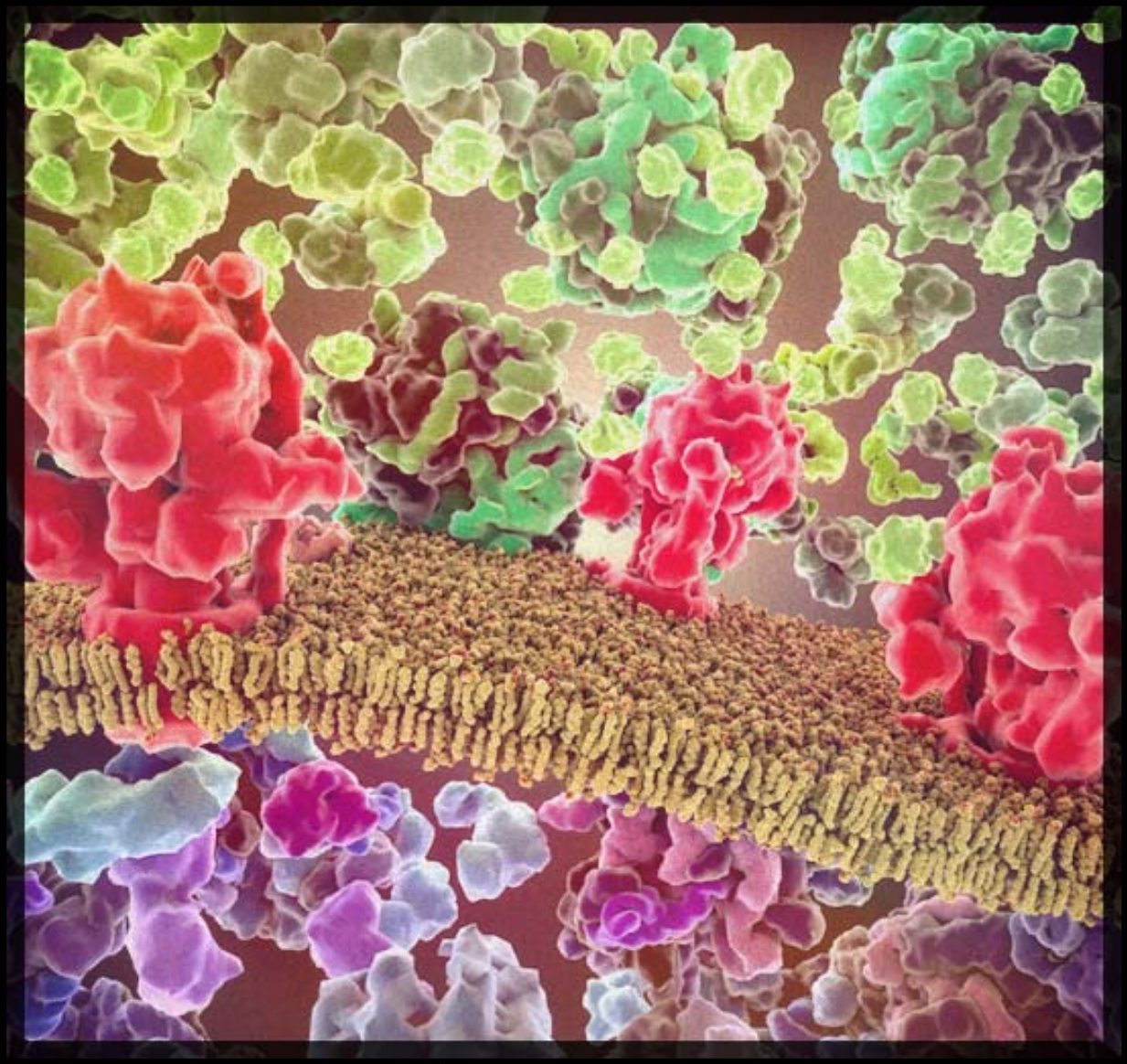

(Adam Gardner)

Virtual Flu

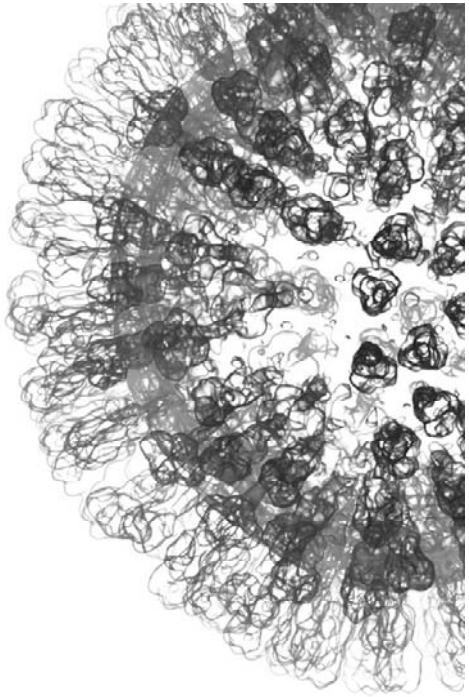

- Introduction
- Model Construction / Tool Development
- **Ongoing simulations**
- Utility

Benchmarking (Stampede)

```
256   0.6 ns/day
512   1.3 ns/day
1024  2.4 ns/day
```

(Intel Xeon Phi coprocessors)

Photo: TACC

BlueWaters: Simulation Benchmarks

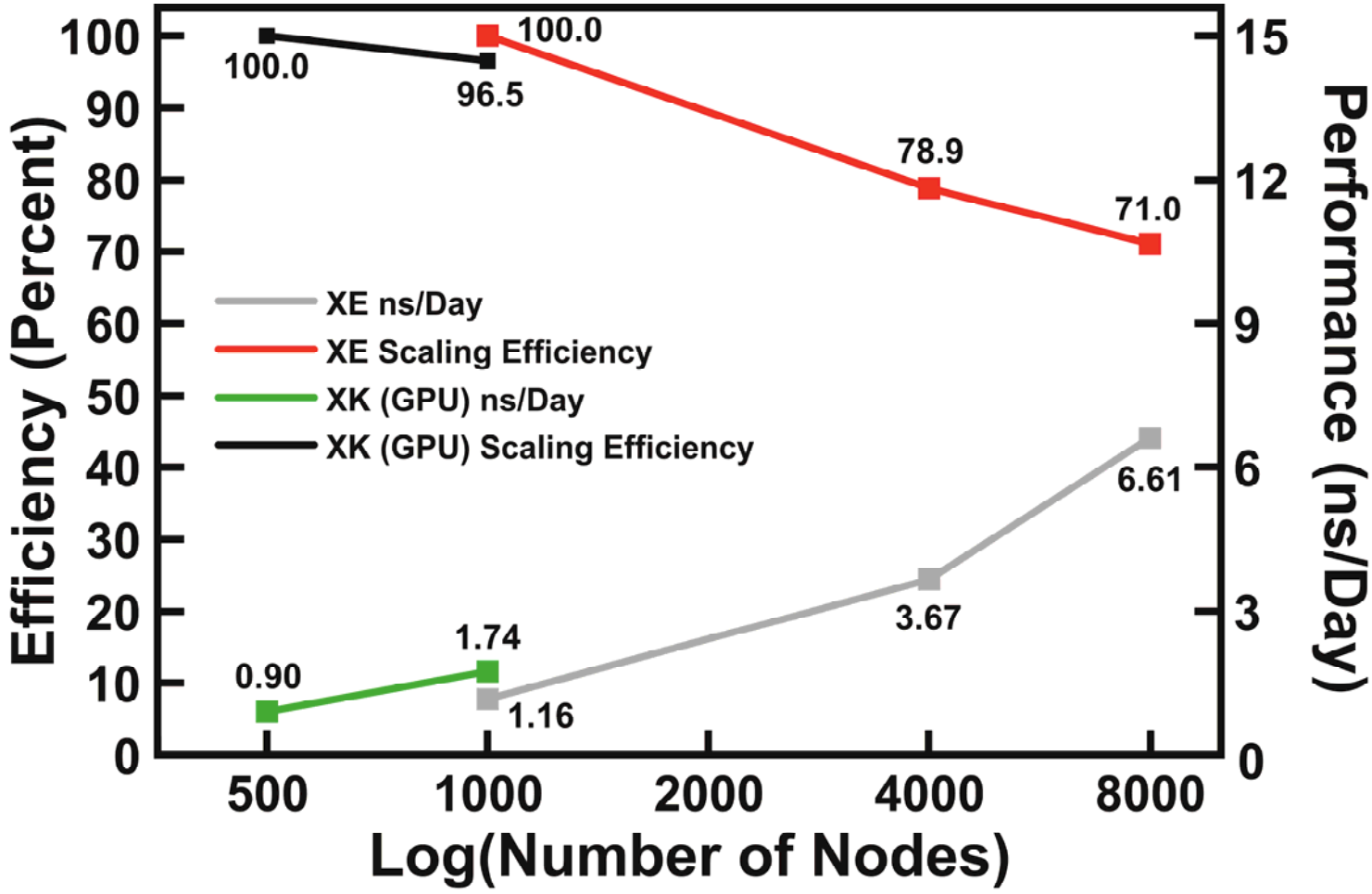

Lipid-Bilayer Instabilities

- After atomic-resolution simulations, instabilities in the bilayer became evident.
- Others have noted similar “holes,” suggesting this challenge is not specific to our system.
- Even the smallest inaccuracies in bilayer densities are amplified many times in mesoscale simulations.

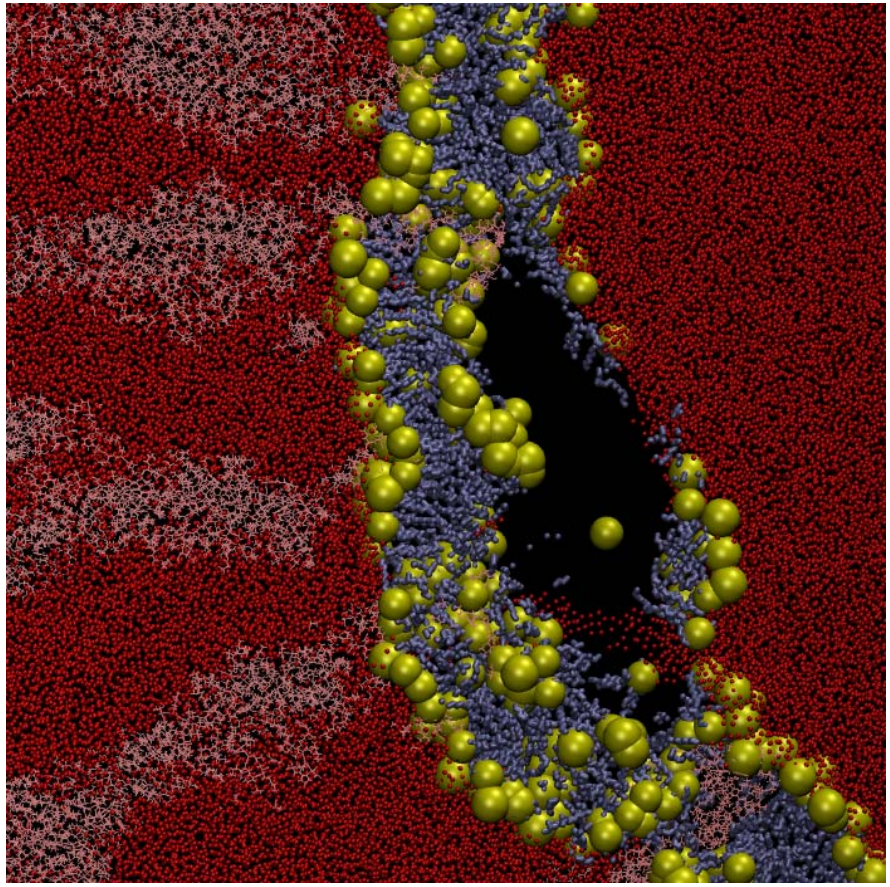

Molecular Dynamics Flexible Fitting

- Define regions of attractive or repulsive potential that are applied over the course of a molecular-dynamics simulation.
- Originally created to allow simulations to be “guided” by densities derived from cryoelectron microscopy.

Zhao, G. P. et al. Mature HIV-1 capsid structure by cryo-electron microscopy and all-atom molecular dynamics. Nature 497, 643-646 (2013).

Trabuco, L. G., Villa, E., Mitra, K., Frank, J. & Schulten, K. Flexible fitting of atomic structures into electron microscopy maps using molecular dynamics. *Structure* **16**, 673-683 (2008).

Bilayer-Repair Procedure

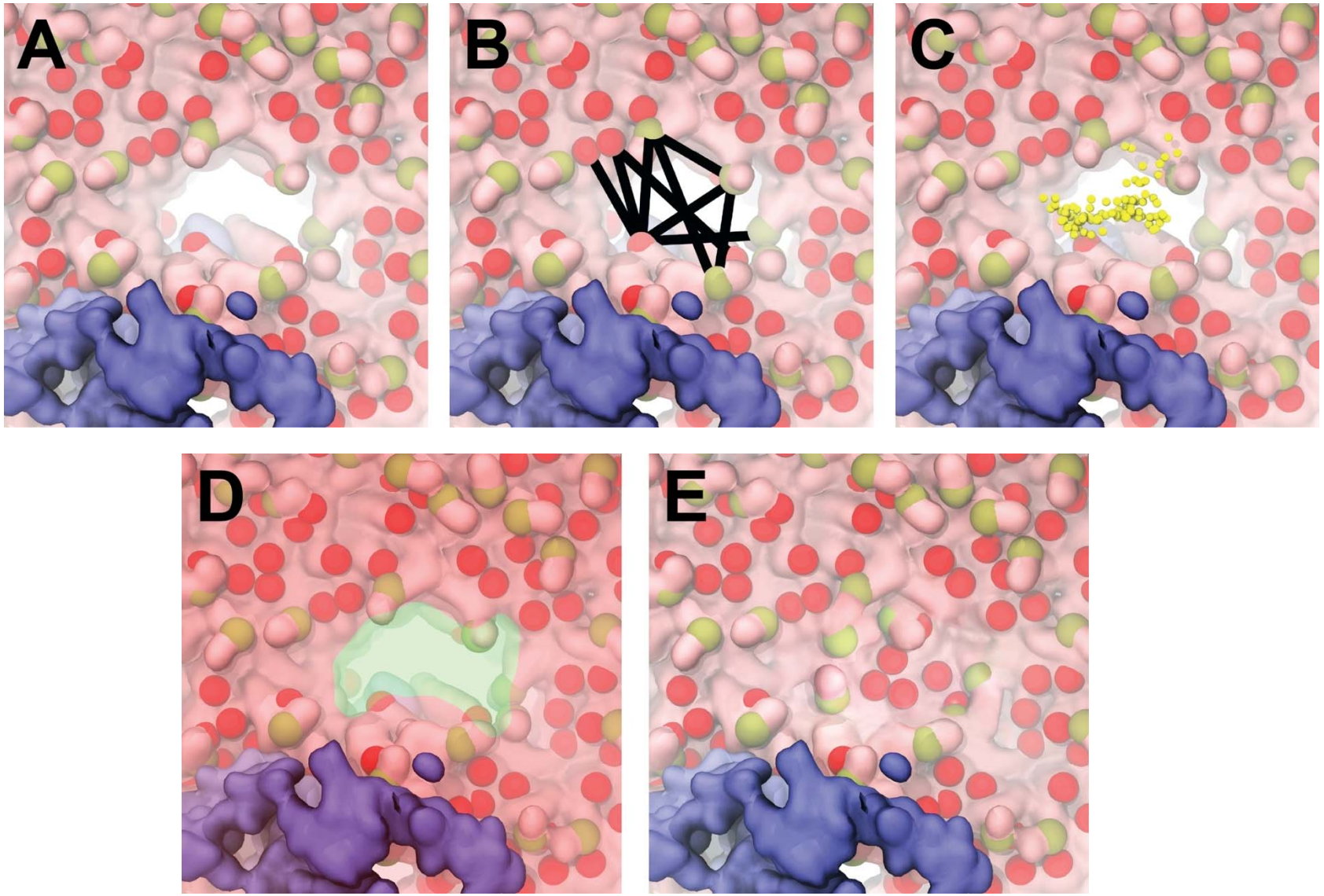

Virtual Flu

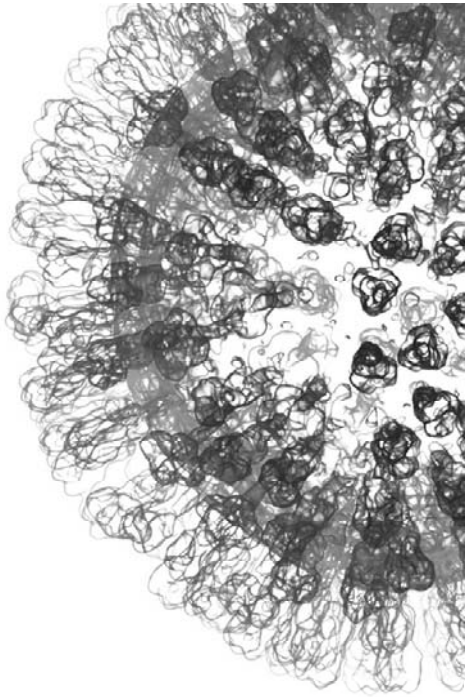

- Introduction
- Model Construction / Tool Development
- Ongoing simulations
- **Utility**

In silico tests might allow us to study influenza strains with pandemic potential, without having to create those strains in the lab.

Time Line: Resurrecting Old Viruses

- 2005: The 1918 “Spanish flu” virus is resurrected.
- 2005: The full genome of the 1918 H1N1 virus is published.
- 2006: The 1918 virus is recreated from publicly available sequences.

Tumpey, T. M. *et al.* Characterization of the reconstructed 1918 Spanish influenza pandemic virus. *Science* **310**, 77-80 (2005)

Taubenberger, J. K. *et al.* Characterization of the 1918 influenza virus polymerase genes. *Nature* **437**, 889-893 (2005)

Kobasa, D. *et al.* Aberrant innate immune response in lethal infection of macaques with the 1918 influenza virus. *Nature* **445**, 319-323 (2007)

Time Line: Gain-of-Function Experiments

- 2009: H9N2-H3N2 reassortment virus with enhanced transmissibility.
- 2011: Transmissible H5N1 strain.
- 2011: A second lab creates a transmissible H5N1 strain.
- 2011: Highly pathogenic H1N1-H5N1 reassortment virus.
- 2011: H9N2-H1N1 reassortment virus with enhanced virulence.
- 2011: H9N2-H1N1 reassortment virus capable of respiratory droplet transmission.

Sorrell, E. M., Wan, H. Q., Araya, Y., Song, H. C. & Perez, D. R. Minimal molecular constraints for respiratory droplet transmission of an avian-human H9N2 influenza A virus. *Proc. Natl. Acad. Sci. U. S. A.* **106**, 7565-7570 (2009)

Imai, M. *et al.* Experimental adaptation of an influenza H5 HA confers respiratory droplet transmission to a reassortant H5 HA/H1N1 virus in ferrets. *Nature* **486**, 420-428 (2012)

Herfst, S. *et al.* Airborne Transmission of Influenza A/H5N1 Virus Between Ferrets. *Science* **336**, 1534-1541 (2012)

Cline, T. D. *et al.* Increased Pathogenicity of a Reassortant 2009 Pandemic H1N1 Influenza Virus Containing an H5N1 Hemagglutinin. *Journal of Virology* **85**, 12262-12270 (2011)

Sun, Y. P. *et al.* High genetic compatibility and increased pathogenicity of reassortants derived from avian H9N2 and pandemic H1N1/2009 influenza viruses. *Proc. Natl. Acad. Sci. U. S. A.* **108**, 4164-4169 (2011)

Kimble, J. B., Sorrell, E., Shao, H. X., Martin, P. L. & Perez, D. R. Compatibility of H9N2 avian influenza surface genes and 2009 pandemic H1N1 internal genes for transmission in the ferret model. *Proc. Natl. Acad. Sci. U. S. A.* **108**, 12084-12088 (2011)

Time Line: Gain-of-Function Experiments

- 2012: H9N2-H1N1 reassortment virus with enhanced replication and transmissibility.
- 2013: H5N1 HA modified to make the virus more transmissible.
- 2013: H5N1-H1N1 reassortment virus with enhanced transmissibility.
- 2014: A highly pathogenic virus similar to the 1918 H1N1 strain.
- 2014: H7N9 is modified to be airborne transmissible in a mammalian host.

Qiao, C. L. *et al.* Pathogenicity and transmissibility of reassortant H9 influenza viruses with genes from pandemic H1N1 virus. *J Gen Virol* **93**, 2337-2345 (2012)

Shelton, H., Roberts, K. L., Molesti, E., Temperton, N. & Barclay, W. S. Mutations in haemagglutinin that affect receptor binding and pH stability increase replication of a PR8 influenza virus with H5 HA in the upper respiratory tract of ferrets and may contribute to transmissibility. *J Gen Virol* **94**, 1220-1229 (2013)

Zhang, Y. *et al.* H5N1 Hybrid Viruses Bearing 2009/H1N1 Virus Genes Transmit in Guinea Pigs by Respiratory Droplet. *Science* **340**, 1459-1463 (2013)

Watanabe, T. *et al.* Circulating Avian Influenza Viruses Closely Related to the 1918 Virus Have Pandemic Potential. *Cell Host Microbe* **15**, 692-705 (2014)

Sutton, T. C. *et al.* Airborne Transmission of Highly Pathogenic H7N1 Influenza Virus in Ferrets. *Journal of Virology* **88**, 6623-6635 (2014)

Time Line

- 1977: An H1N1 pandemic breaks out in China and Russia. It is genetically identical to a 27-year-old 1950 strain. Some speculate it was accidentally released from a laboratory specimen.
- 2014: The CDC accidentally contaminates a sample of non-pathogenic influenza with highly pathogenic H5N1 and ships the sample to an outside USDA laboratory.
  - This accident was only discovered because they were investigating a similar anthrax accident.

Webster, R. G., Bean, W. J., Gorman, O. T., Chambers, T. M. & Kawaoka, Y. Evolution and Ecology of Influenza-a Viruses. *Microbiol Rev* **56**, 152-179 (1992)

Lipsitch, M. & Galvani, A. P. Ethical Alternatives to Experiments with Novel Potential Pandemic Pathogens. *Plos Med* **11** (2014)

Ennis, F. A. Influenza-a Viruses - Shaking out Our Shibboleths. *Nature* **274**, 309-310 (1978)

Nakajima, K., Desselberger, U. & Palese, P. Recent Human Influenza-a (H1n1) Viruses Are Closely Related Genetically to Strains Isolated in 1950. *Nature* **274**, 334-339 (1978)

CDC Director Releases After-Action Report on Recent Anthrax Incident; Highlights Steps to Improve Laboratory Quality and Safety (CDC, Atlanta, Georgia, 2014)

Neuman, S. CDC Closes Two Labs After Anthrax, Flu Scares. *NPR* (2014)

Modeling the Electrostatic Environment

- The electrostatic field surrounding the virion likely has a profound impact on virulence.
  - The HA binding domain has increased positive potential in human- vs. avian-adapted H3.
  - Phylogenetic analysis of H3N2 shows an increase in net positive charge over the course of HA evolution in humans.

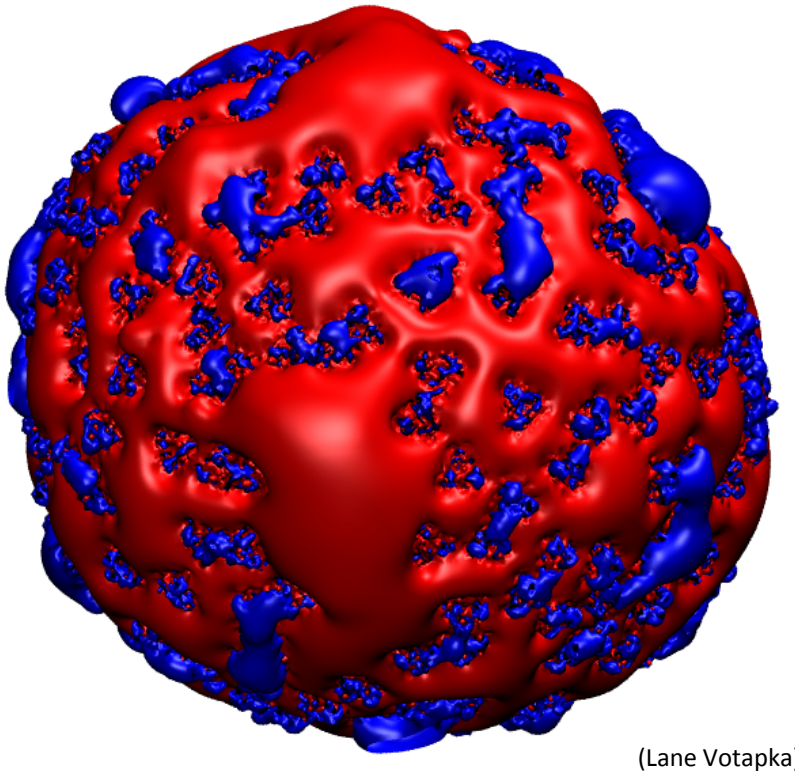

(Lane Votapka)

Newhouse, E. I.; Xu, D.; Markwick, P. R.; Amaro, R. E.; Pao, H. C.; Wu, K. J.; Alam, M.; McCammon, J. A.; Li, W. W. Mechanism of glycan receptor recognition and specificity switch for avian, swine, and human adapted influenza virus hemagglutinins: a molecular dynamics perspective. *J. Am. Chem. Soc.* **2009***,* 131 (47), 17430.

Kobayashi, Y.; Suzuki, Y. Compensatory evolution of net-charge in influenza A virus hemagglutinin. *PloS one* **2012***,* 7 (7), e40422.

Stalk Height Impacts Electrostatics

- Recent highly pathogenic H7N9 contains a five amino-acid NA stalk deletion that is correlated with increased virulence in other strains.
- Affects the NA height and, therefore, the resulting electrostatic properties of the virion.

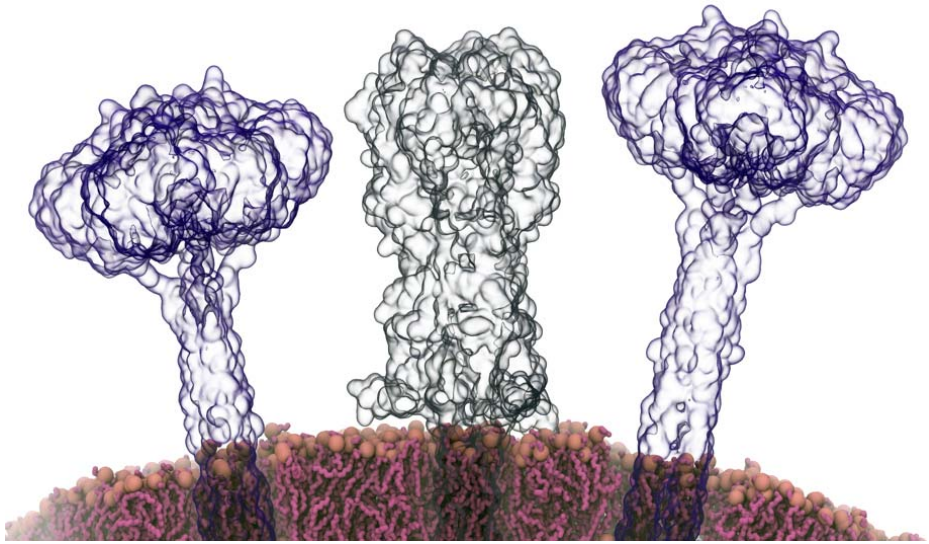

Gao, R.; Cao, B.; Hu, Y.; Feng, Z.; Wang, D.; Hu, W.; Chen, J.; Jie, Z.; Qiu, H.; Xu, K.; Xu, X.; Lu, H.; Zhu, W.; Gao, Z.; Xiang, N.; Shen, Y.; He, Z.; Gu, Y.; Zhang, Z.; Yang, Y.; Zhao, X.; Zhou, L.; Li, X.; Zou, S.; Zhang, Y.; Li, X.; Yang, L.; Guo, J.; Dong, J.; Li, Q.; Dong, L.; Zhu, Y.; Bai, T.; Wang, S.; Hao, P.; Yang, W.; Zhang, Y.; Han, J.; Yu, H.; Li, D.; Gao, G. F.; Wu, G.; Wang, Y.; Yuan, Z.; Shu, Y. Human infection with a novel avian-origin influenza A (H7N9) virus. *The New England journal of medicine* **2013***,* 368 (20), 1888.

Matsuoka, Y.; Swayne, D. E.; Thomas, C.; Rameix-Welti, M. A.; Naffakh, N.; Warnes, C.; Altholtz, M.; Donis, R.; Subbarao, K. Neuraminidase stalk length and additional glycosylation of the hemagglutinin influence the virulence of influenza H5N1 viruses for mice. *J Virol* **2009***,* 83 (9), 4704.

Pharmacological Implications

- Simulations will provide pharmacologically relevant insights into glycoprotein flexibility.
- The “microscopic milieu” may well affect binding-pocket dynamics.
- Dynamics on the order of 100 ns are known to reveal novel influenza-glycoprotein druggable binding sites.

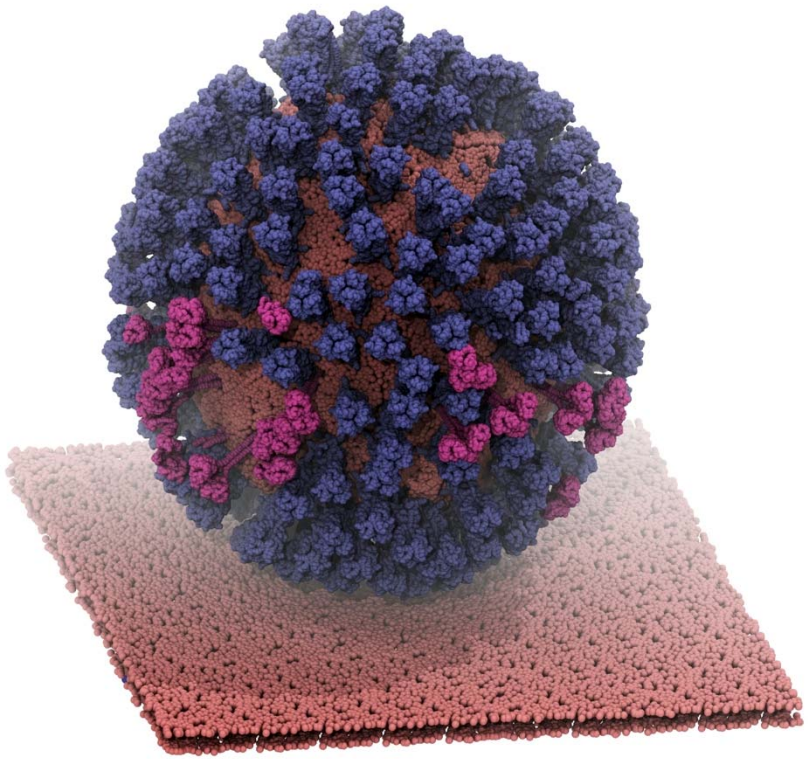

Acknowledgements

- Amaro Lab
  - Lane Votapka
  - Rommie E. Amaro
- Theoretical and Computational Biophysics Group (UIUC)
  - Juan Perilla
  - Abhi Singharoy
  - Jim Phillips
  - John Stone
  - Danielle Chandler
  - Klaus Schulten
- Many other wonderful collaborators

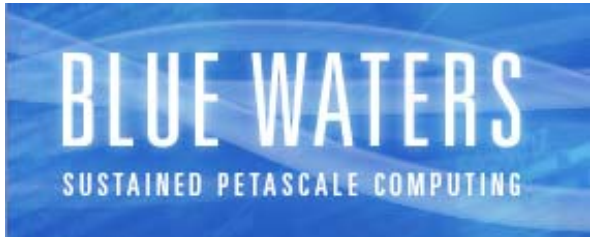

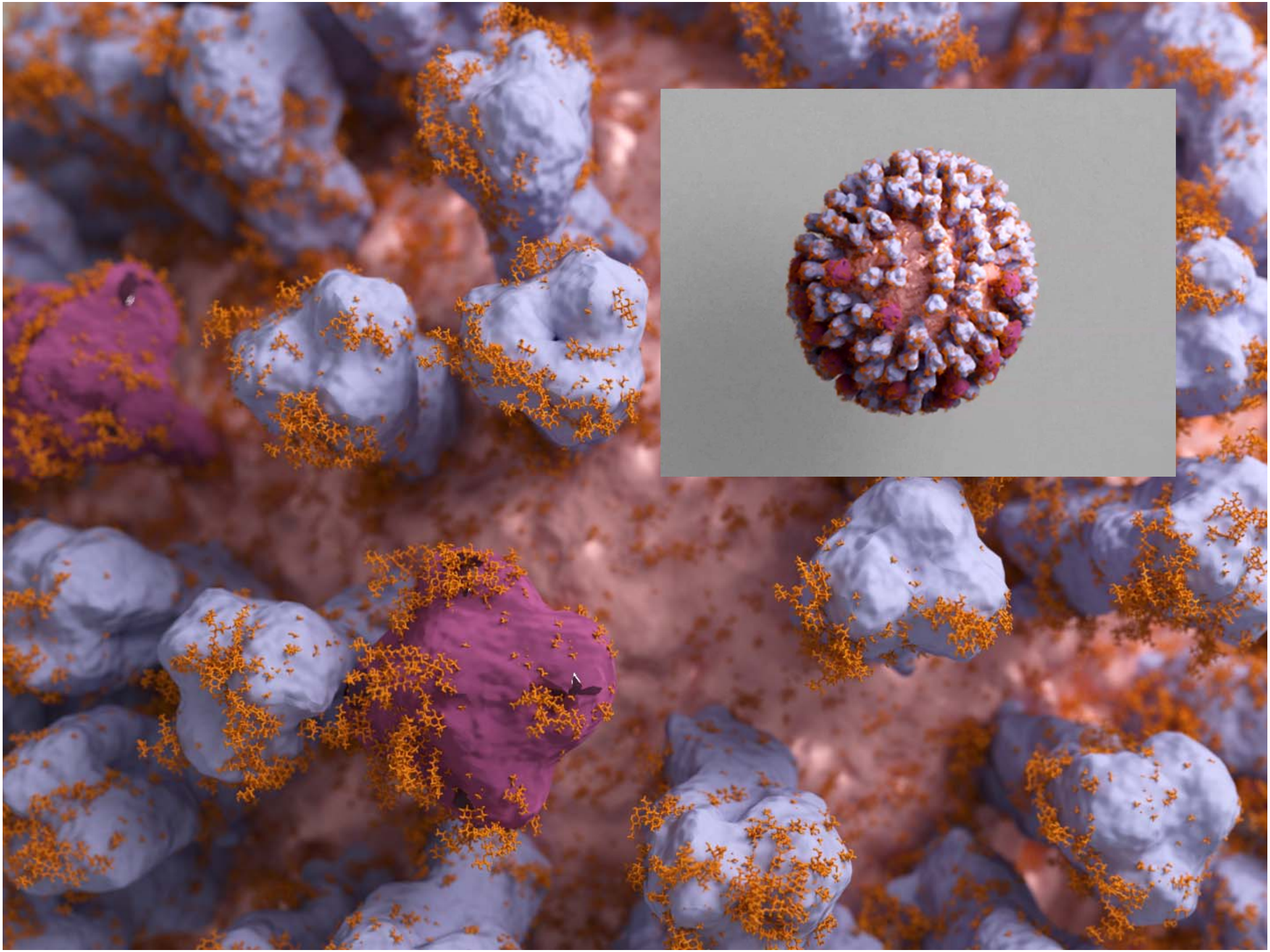

LipidWrapper as a Software Component

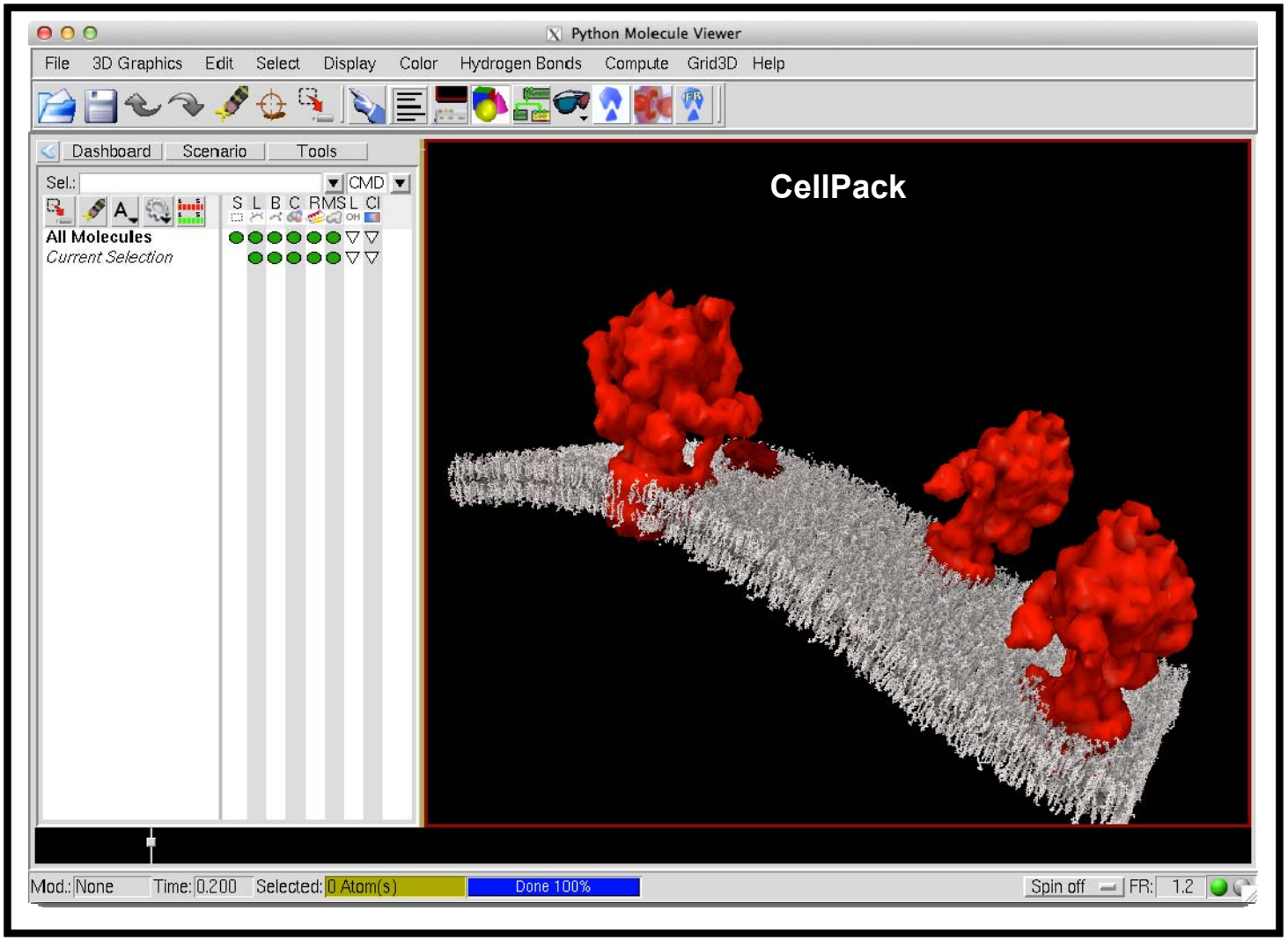

Overview: Model Construction

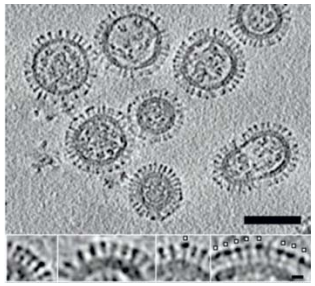

Cryo-electron tomography data from Alasdair Steven, NIH

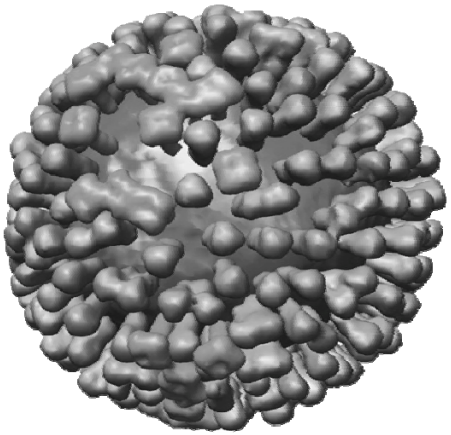

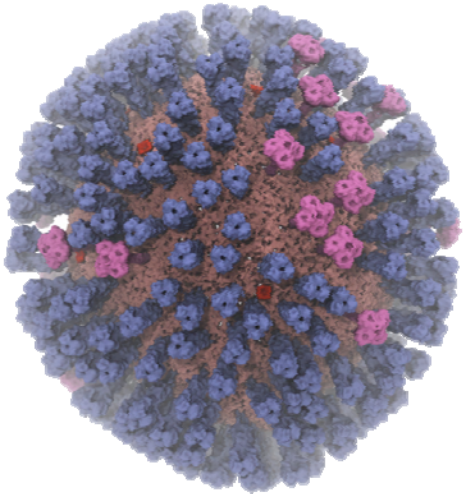

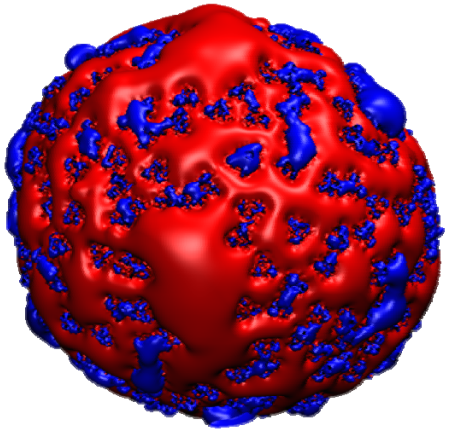

Influenza Description

- Enveloped RNA virus: eight ribonucleoproteins surrounded by a lipid membrane.
- Hemagglutinin (HA) and neuraminidase (NA) protrude roughly 15 nanometers: ectodomains + filamentous stalks.
- M2 proton channels.

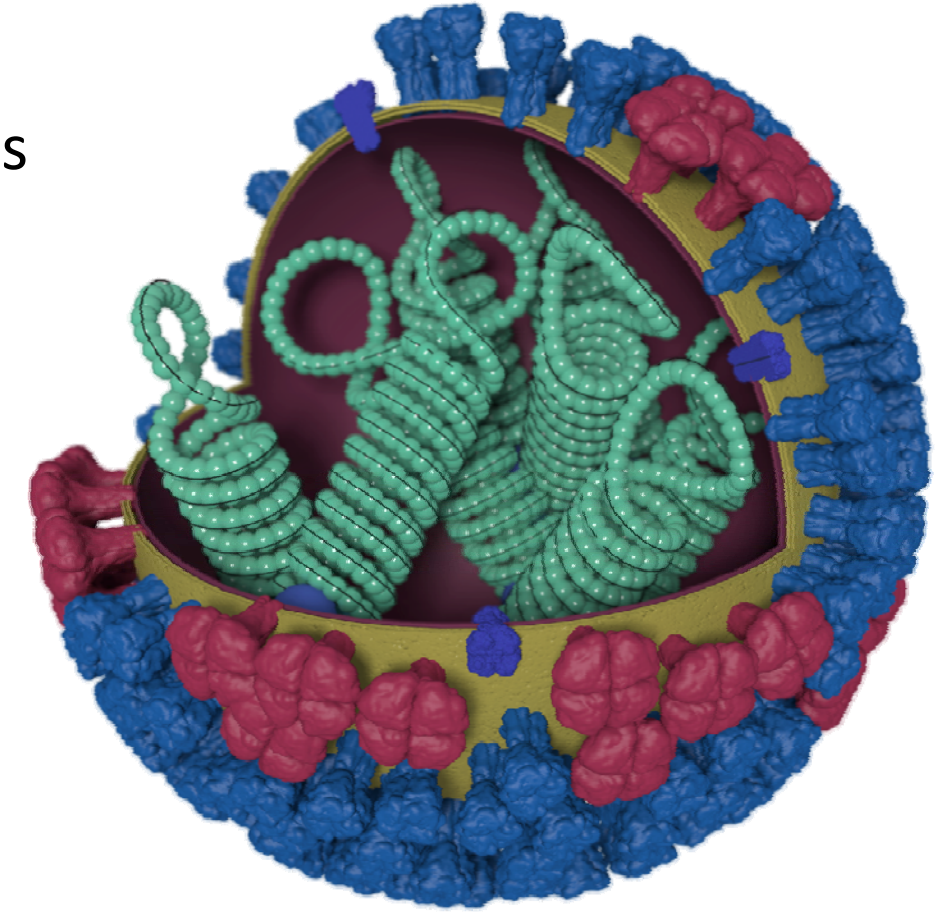

Photo Credit: Dan Higgins

To Answer Specific Questions about Model Construction

NA Ectodomain Monomer

- NA is a tetramer.
- Homology model of a single monomer.
  - 2009 H1N1 pandemic NA sequence (A/California/04/2009).
  - 3NSS crystal structure (also 2009 H1N1).
  - Schrödinger Prime.

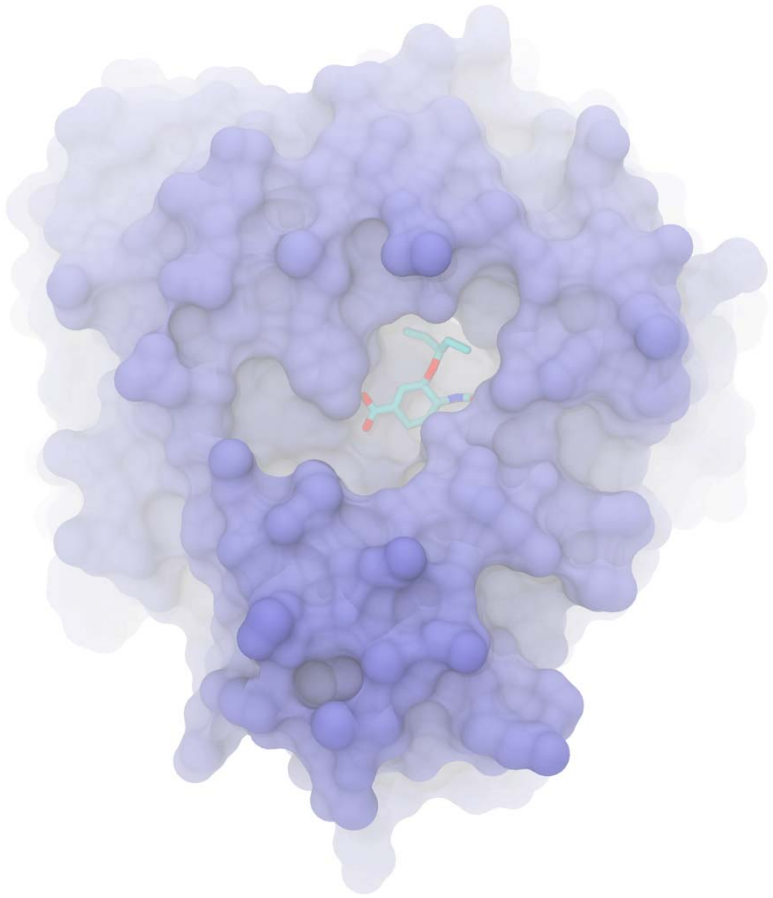

Li, Q. *et al.* The 2009 pandemic H1N1 neuraminidase N1 lacks the 150-cavity in its active site. *Nat Struct Mol Biol* **17**, 1266-1268

NA Ectodomain Tetramer

- Copied and aligned monomer to each chain of 2HU4 (Multiseq in VMD).

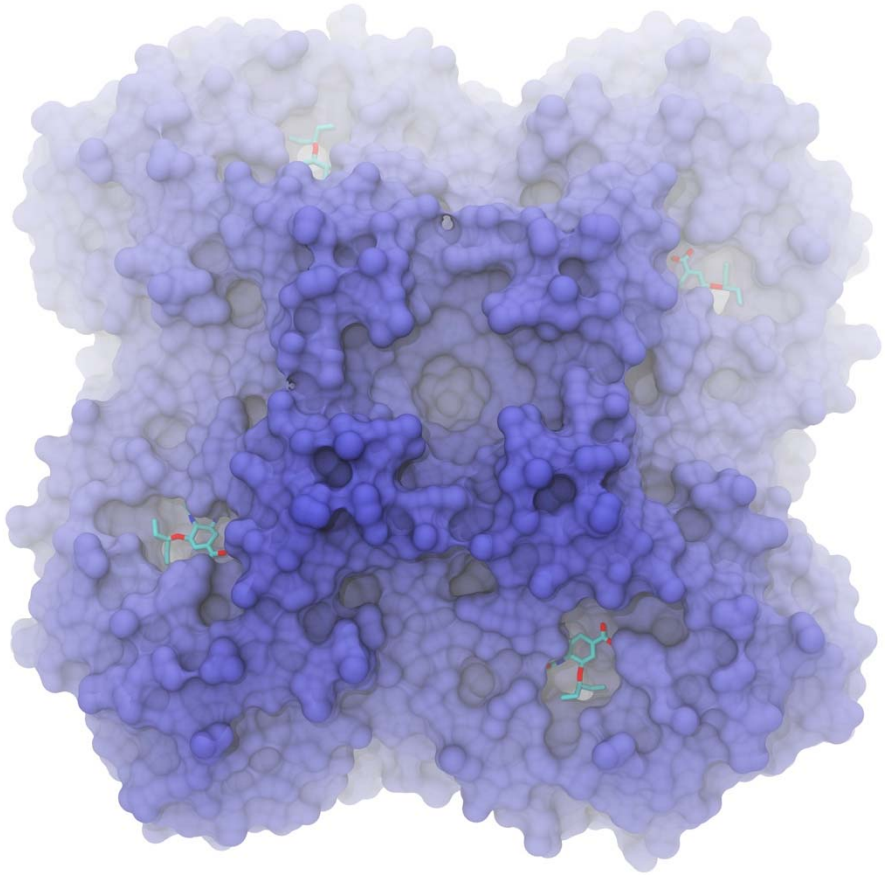

Humphrey, W., Dalke, A. & Schulten, K. VMD: visual molecular dynamics. *J. Mol. Graphics* **14**, 33-38

Roberts, E., Eargle, J., Wright, D. & Luthey-Schulten, Z. MultiSeq: unifying sequence and structure data for evolutionary analysis. *BMC Bioinf.* **7**, 382 (2006).

Russell, R. J. *et al.* The structure of H5N1 avian influenza neuraminidase suggests new opportunities for drug design. *Nature* **443**, 45-49

NA Stalk

- Alpha helical, but no crystal structure.
- Created alpha helix with appropriate sequence in Amber XLEAP.
- RosettaDock 3.4 to assemble this helix into a four-helix bundle, one helix at a time.
  - ~100,000 dockings each round
  - Clustering and visual inspection to identify acceptable poses.

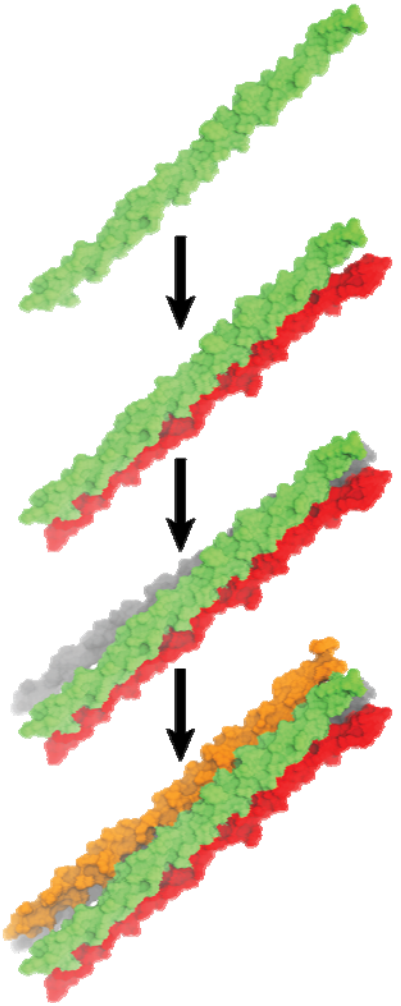

Case, D. *et al.* AMBER 12. *University of California, San Francisco* (2012).

Chaudhury, S., Sircar, A., Sivasubramanian, A., Berrondo, M. & Gray, J. J. Incorporating biochemical information and backbone flexibility in RosettaDock for CAPRI rounds 6-12. *Proteins-Structure Function and Bioinformatics* **69**, 793-800 (2007).

NA Assembly

- NA parts assembled into single whole.
- Embedded in a physiologically relevant planar lipid bilayer built with CHARMM-GUI.

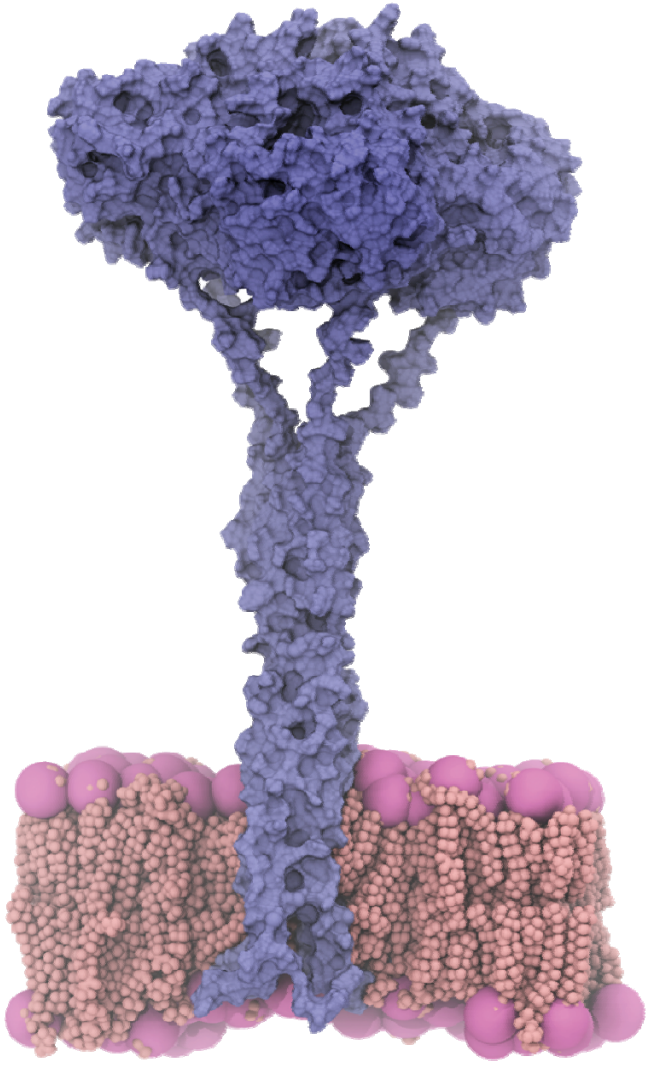

Jo, S., Lim, J. B., Klauda, J. B. & Im, W. CHARMM-GUI Membrane Builder for mixed bilayers and its application to yeast membranes. *Biophys. J.* **97**, 50-58 (2009).

HA Assembly

- Hemagglutinin (HA) was similarly constructed.

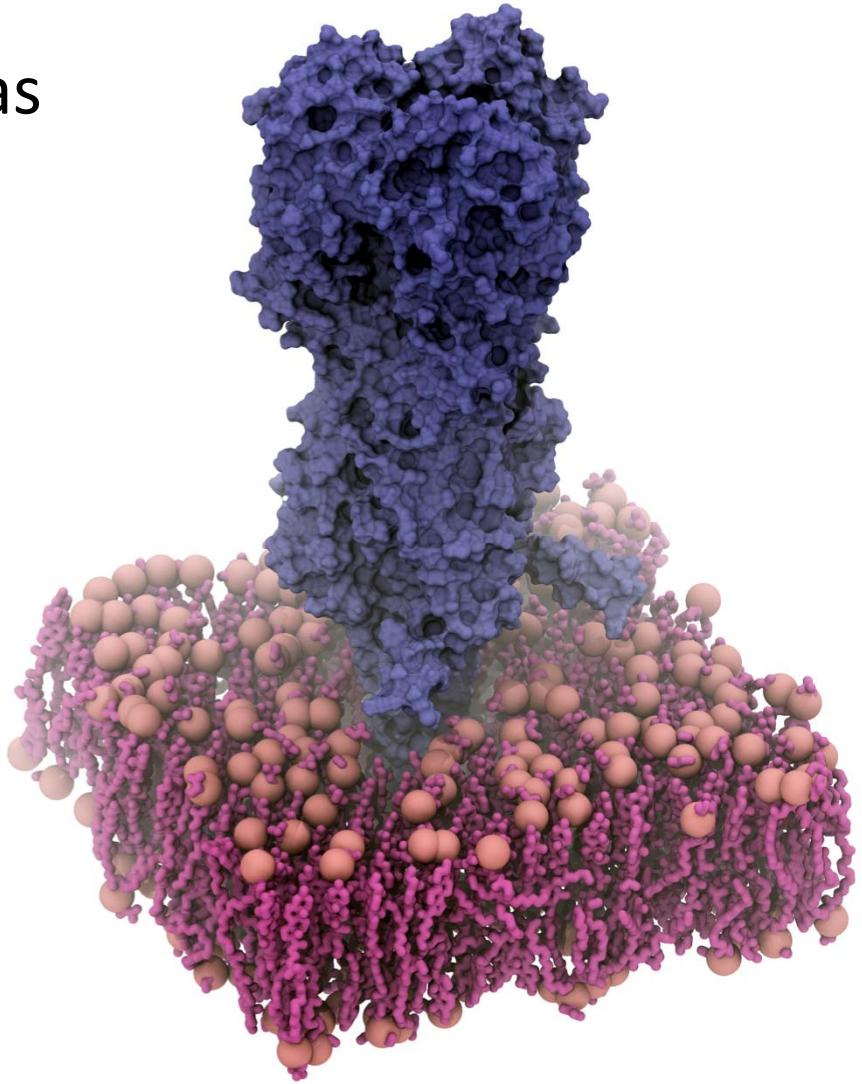

Single Glycoprotein Simulations

Each system: After equilibration, five 100 ns simulations. Clustering ➔ five representative conformations each.

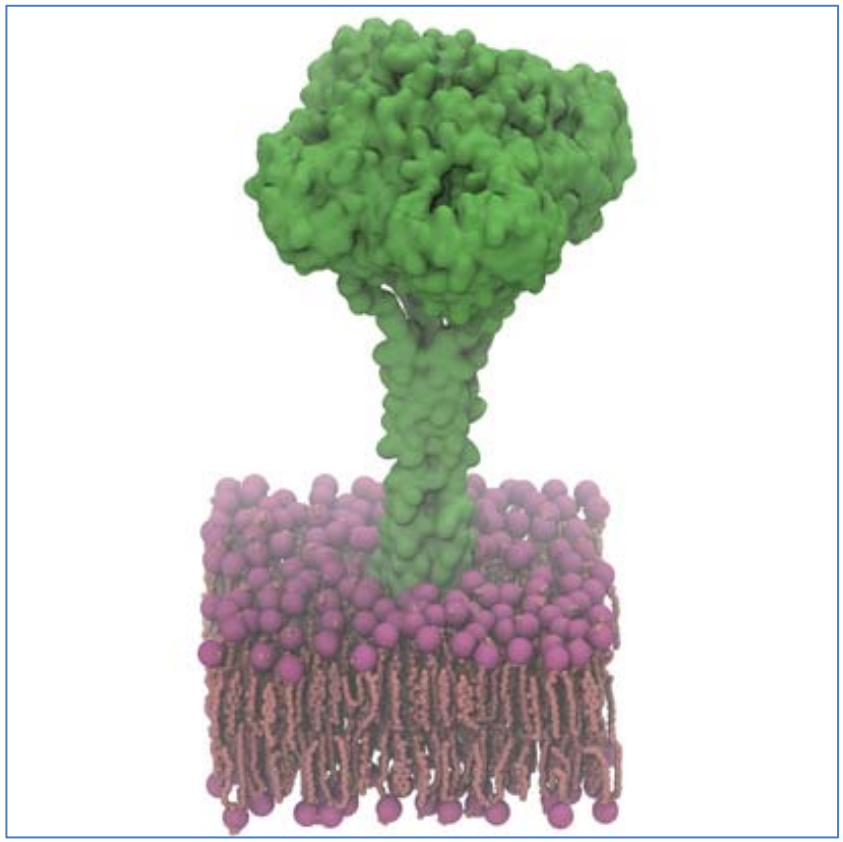

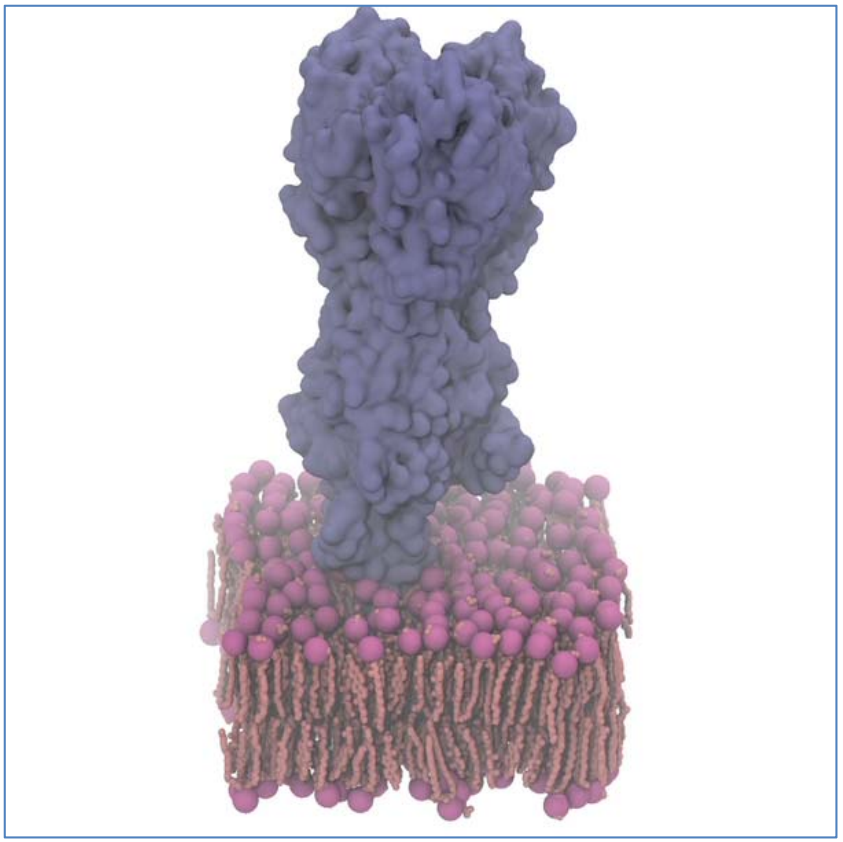

Step 1: Cryoelectron Tomography

- **Cryoelectron tomography was used to determine the general shape of the influenza virion coat.**
- **Resolution: 5.5 nm**

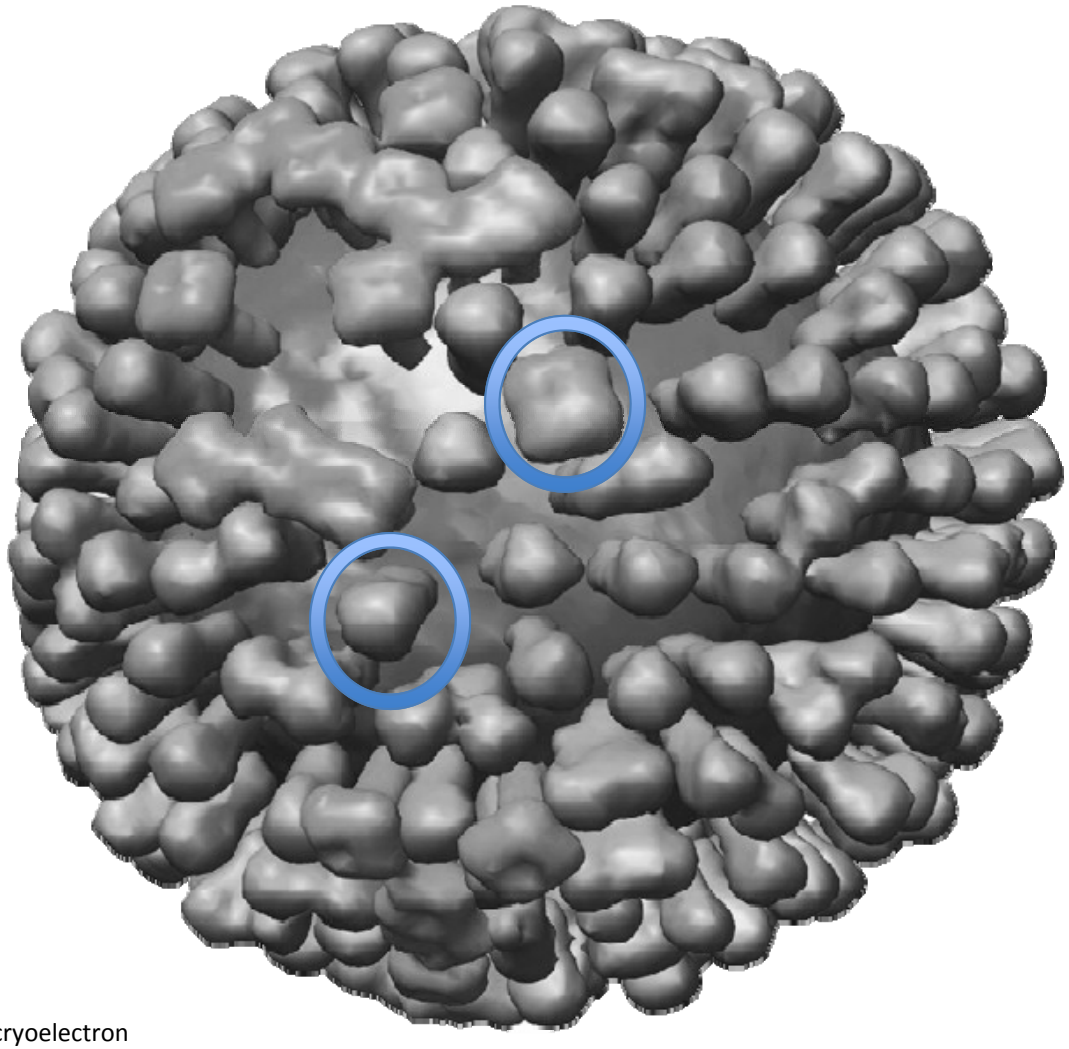

Harris, A. *et al.* Influenza virus pleiomorphy characterized by cryoelectron tomography. *Proc.Natl.Acad.Sci.U.S.A.* **103**, 19123-19127 (2006).

Step 2: A Simplified Point Model

From this model, collaborators generated a simplified point model

- The lipid envelope
- Neuraminidase and hemagglutinin glycoproteins.

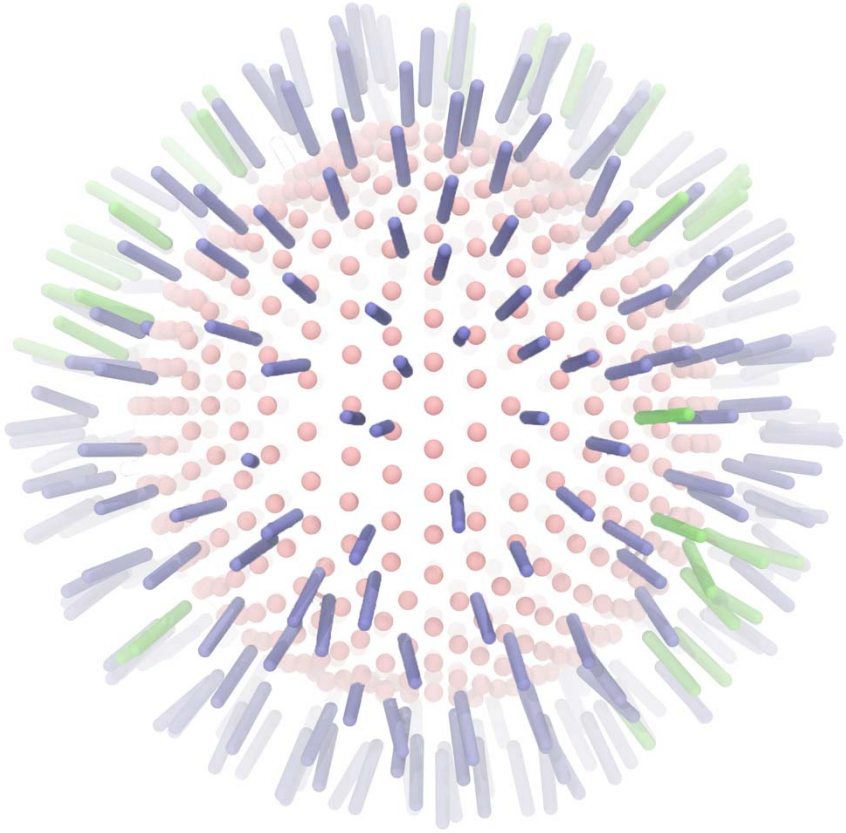

Step 3: Positioning the Glycoproteins

- **PyMolecule: programmatically position atomistic glycoprotein models extracted from simulations**

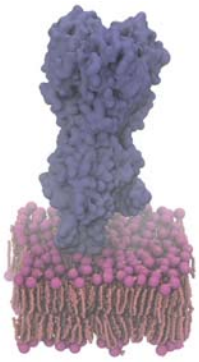

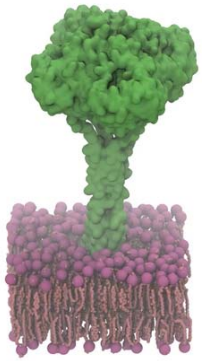

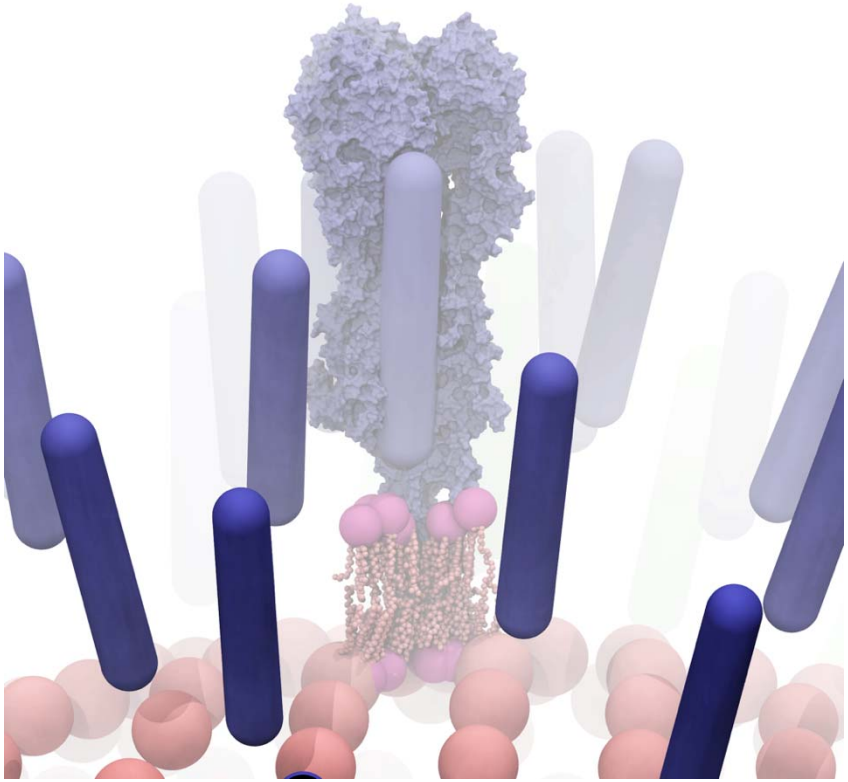

Step 4: A Lipid “Carpet”

- **The points defining the viral envelope were next tessellated/triangulated.**
- **PyMolecule was used to carpet the surface with physiologically relevant lipid-bilayer models.**

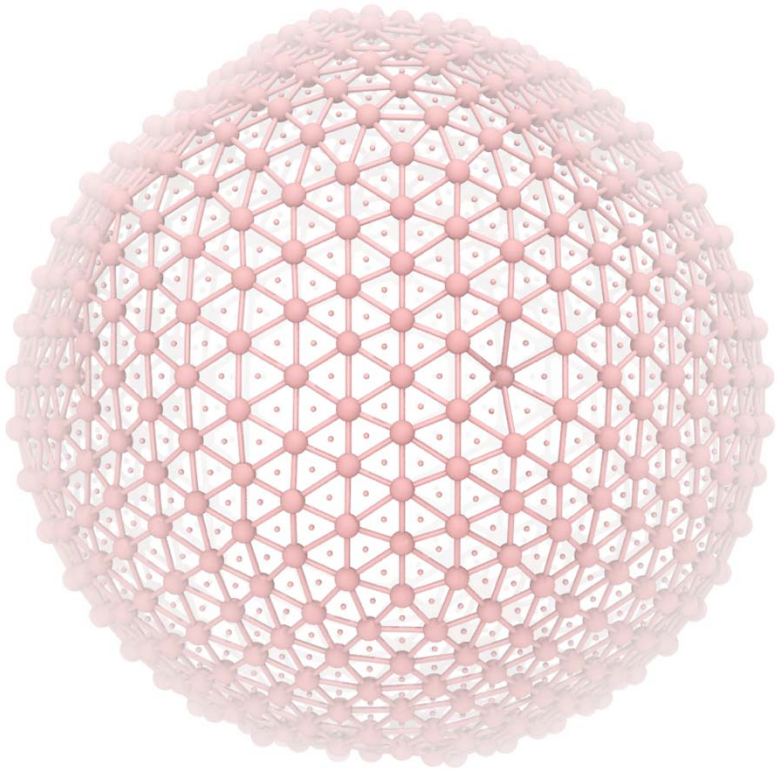

Slides to use if you need more time

Computational Details

- Parameterization
  - CHARMM36: lipids/cholesterol/carbohydrates
  - CHARMM27: proteins
  - TIP3P
- Simulation Details
  - 2.0 fs time step
  - Constant pressure/temperature
  - Memory-optimized version of NAMD2 2.9

Klauda, J. B., Monje, V., Kim, T. & Im, W. Improving the CHARMM Force Field for Polyunsaturated Fatty Acid Chains. J. Phys. Chem. B 116, 9424-9431 (2012).

Klauda, J. B. et al. Update of the CHARMM all-atom additive force field for lipids: validation on six lipid types. J. Phys. Chem. B 114, 7830-7843 (2010).

A “Computational Microscope”

Modeling can serve as a “computational microscope” that bridges the gap between cryo-electron microscopy and x-ray crystallography/NMR .

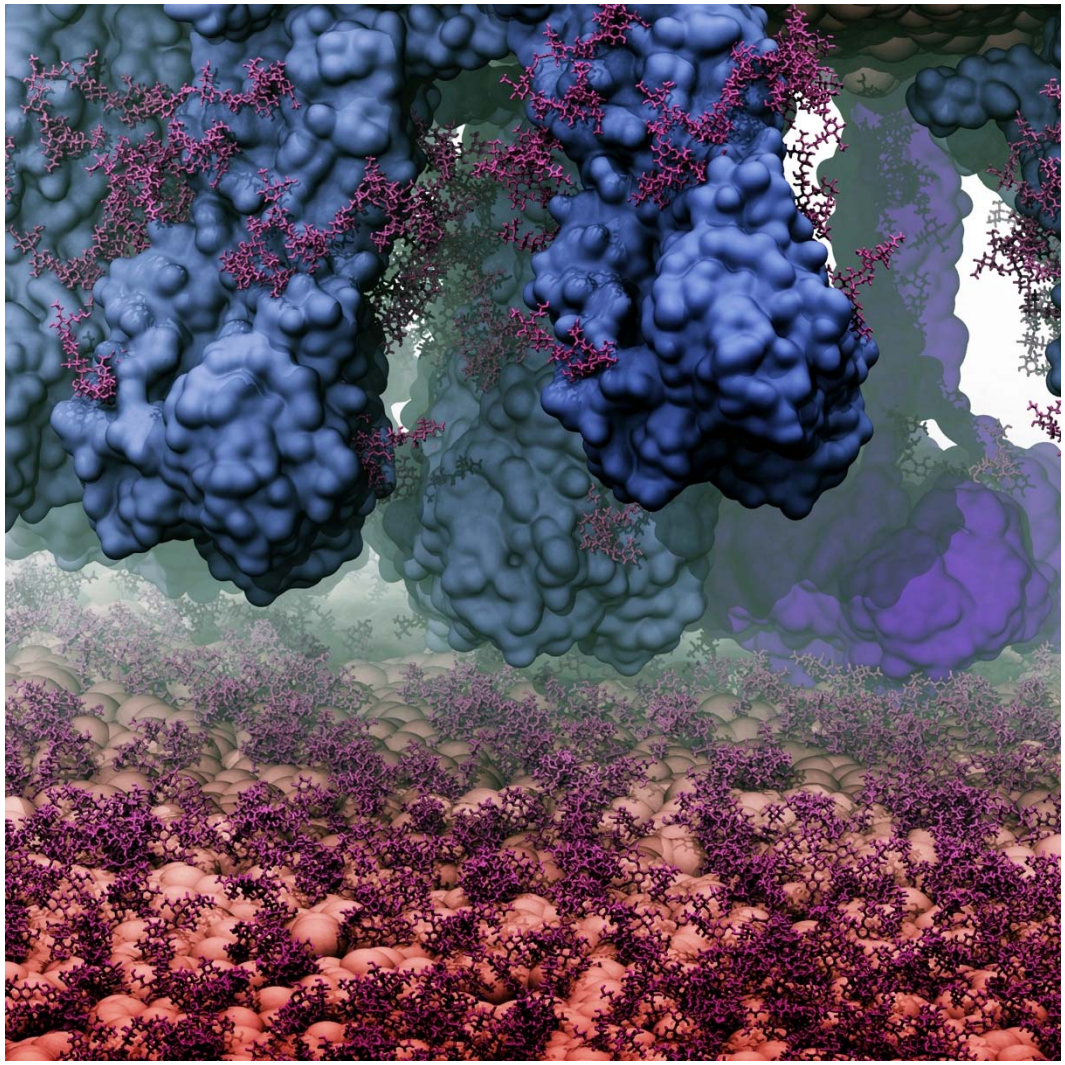

Modeling: A Powerful Tool

- **The power of this "computational microscope" is becoming more well known.**
- **Guided by electron microscopy and x-ray crystallography, our collaborators recently modeled and simulated the entire HIV capsid (64 million atoms).**
  - **"The complete atomic HIV-1 capsid model provides a platform for further studies of capsid function and for targeted pharmacological intervention."**

Zhao, G. P. et al. Mature HIV-1 capsid structure by cryo-electron microscopy and all-atom molecular dynamics. Nature 497, 643-646 (2013).